Current Biology, Volume *29*

Supplemental Information

Inverse Control of Turning Behavior by Dopamine D1 Receptor Signaling in Columnar and Ring Neurons of the Central Complex in *Drosophila*

Benjamin Kottler, Richard Faville, Jessika Cristina Bridi, and Frank Hirth

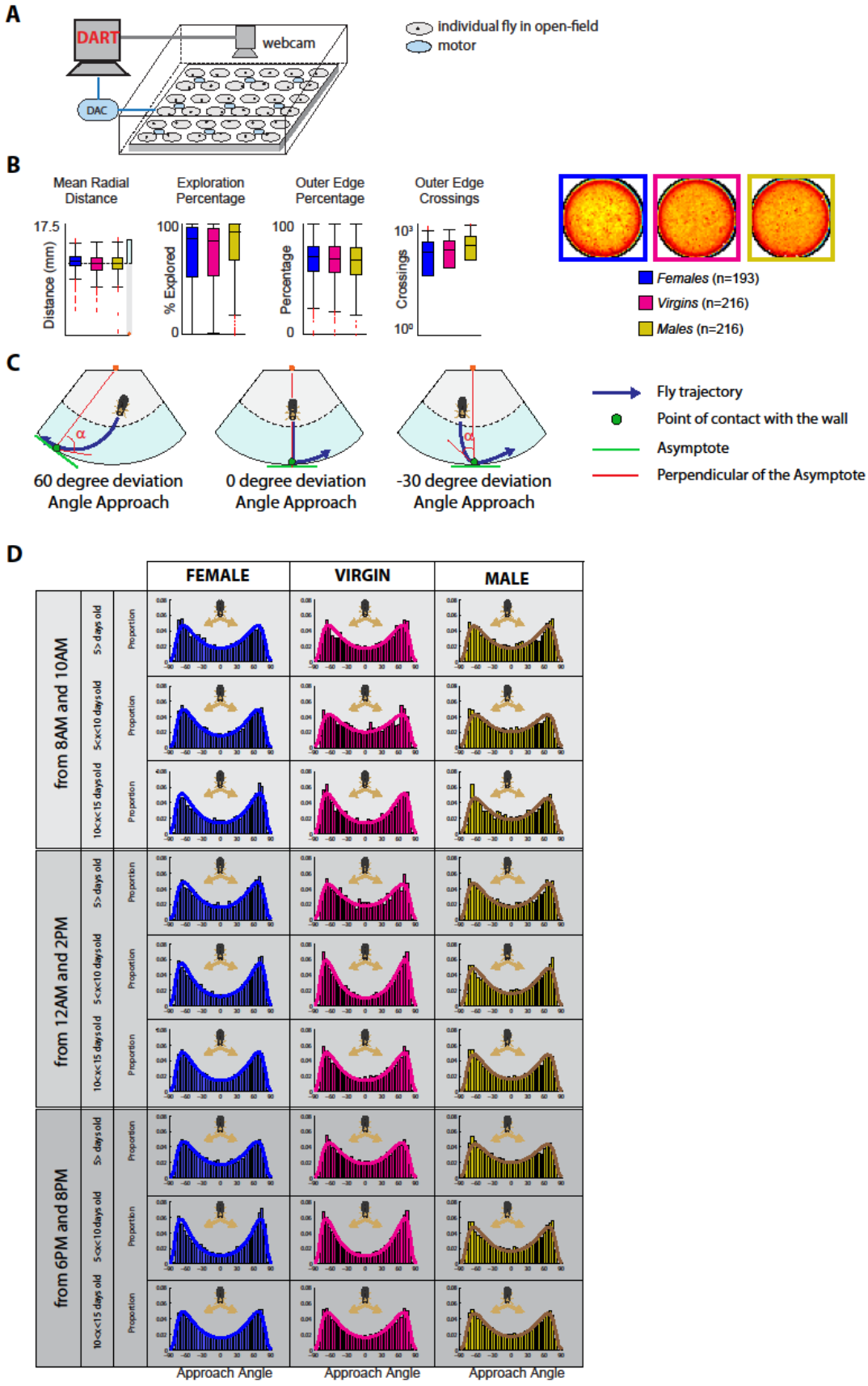
A
DART
webcam
DAC
individual fly in open-field
motor
B
Mean Radial Distance
Exploration Percentage
Outer Edge Percentage
Outer Edge Crossings
17.5
Distance (mm)
100
% Explored
0
100
Percentage
0
10³
Crossings
10⁰
Females (n=193)
Virgins (n=216)
Males (n=216)
C
60 degree deviation Angle Approach
0 degree deviation Angle Approach
-30 degree deviation Angle Approach
Fly trajectory
Point of contact with the wall
Asymptote
Perpendicular of the Asymptote
D
FEMALE
VIRGIN
MALE
from 8AM and 10AM
from 12AM and 2PM
from 6PM and 8PM
5> days old
5<x<10 days old
10<x<15 days old
Proportion
Approach Angle

Figure S1: Open-field behaviour of freely moving controls flies. Relates to Figure 1. (**A**) Behavioural setup; platform with 36 open-field arenas, each hosting one fly, placed in a temperature-controlled incubator; all experimental and control flies were tracked at the same time. DART software was used for controlling the webcam and the motor, via a digital to analogue converter (DAC); motor activation elicits a vibration shock. (**B**) Place preference metrics for control groups, w^{1118} females, virgins and males. (**C**) Schematics of turning behaviour: left, the fly approaches the edge making a sharp clockwise turn to the its right; middle, the fly walks straight to the wall making the turn after contact; right, the fly makes a slight counter clock turn. (**D**) Gender comparison across time of the day and age. Mated females (in blue), virgin females (in pink) and males (in yellow) were compared at different time points of the day and age. In every case, the bimodal distribution is presented with peaks at -/+70degrees and there is no statistical difference between groups.

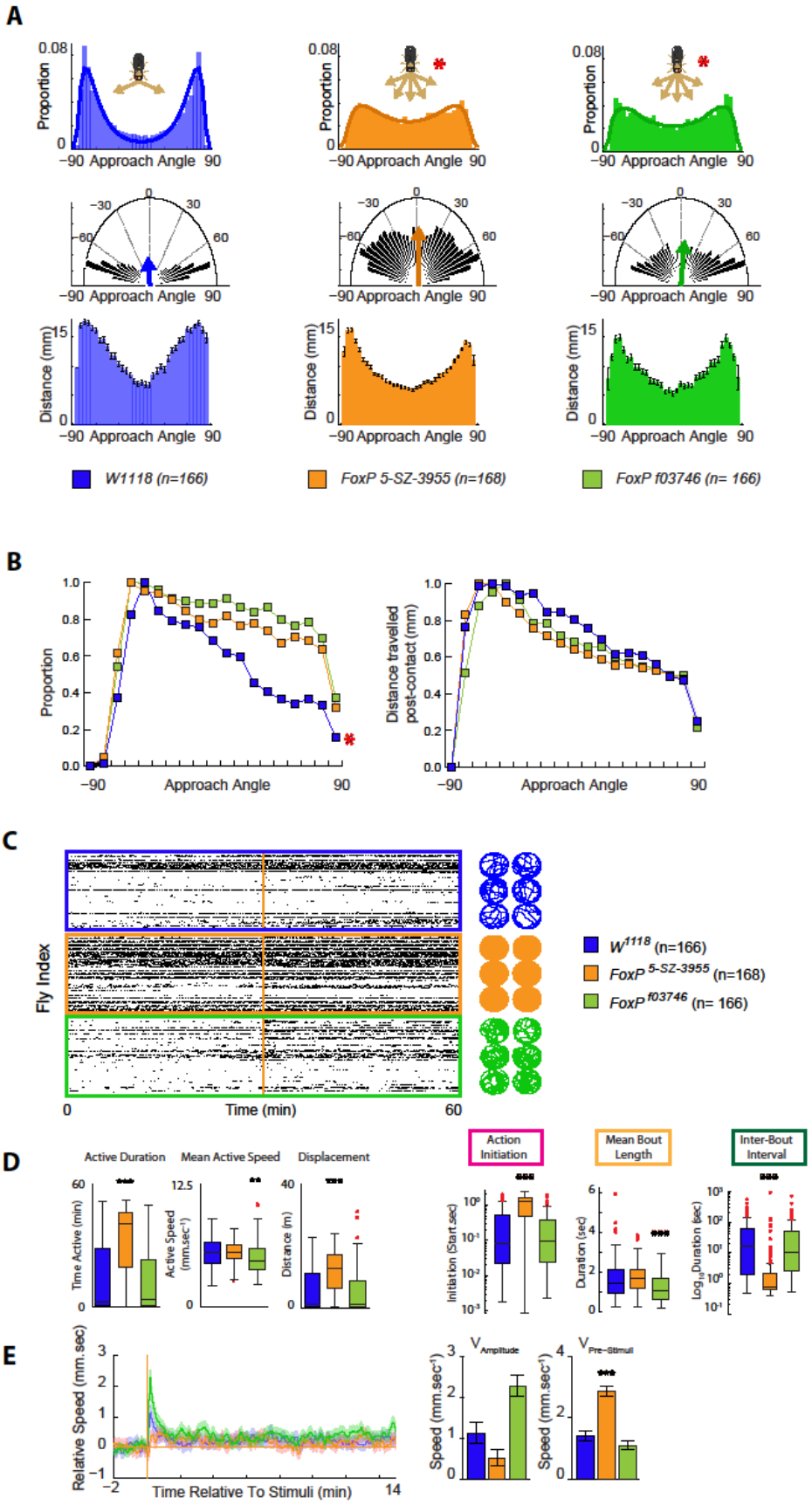
A
Proportion
0.08
0
−90 Approach Angle 90
−30
30
−60
60
0
Distance (mm)
15
W1118 (n=166)
FoxP 5-SZ-3955 (n=168)
FoxP f03746 (n= 166)
B
Proportion
Approach Angle
Distance travelled post-contact (mm)
C
Fly Index
Time (min)
0
60
W1118 (n=166)
FoxP 5-SZ-3955 (n=168)
FoxP f03746 (n= 166)
D
Active Duration
Mean Active Speed
Displacement
Time Active (min)
Active Speed (mm.sec⁻¹)
Distance (m)
Action Initiation
Mean Bout Length
Inter-Bout Interval
Initiation (Start sec)
Duration (sec)
Log10Duration (sec)
E
Relative Speed (mm.sec)
Time Relative To Stimuli (min)
V Amplitude
V Pre-Stimuli
Speed (mm.sec⁻¹)

Figure S2: Locomotor kinematics and open-field behaviour of freely moving *FoxP* mutant flies. Relates to Figure 2. (**A**) approach angle distribution, polar plot representation, and distance travelled post contact with the wall for each group w^{1118} (blue), $FoxP^{5\text{-}SZ\text{-}3955}$ (orange) and $FoxP^{f03746}$ (green) females. (**B**) Left, each approach angle proportion have been grouped based on absolute value and normalized to the maximum; right each distance travelled postcontact with the edge have been grouped based on absolute value and normalized to the maximum. The asterisk represents significant difference with the two other groups based on two sample Kolmogorov-Smirnov (KS). (**C**) Raster plot activity of w^{1118} (blue), $FoxP^{5\text{-}SZ\text{-}3955}$ (orange) and $FoxP^{f03746}$ (green) females; trajectories recorded for the first 10 minutes; panels of the right show activity metrics, mean activity of flies (active duration), their mean active speed (middle) and the distance they walked during the recordings (Displacement). (**D**) Activity metrics related for 60 min recording. (**E)** Relative speed over time before and after stimuli (dashed orange line) are applied; panels on right show stimuli response as amplitude of increased speed after stimuli and pre-stimuli speed. All data are mean +/- SEM; *p<0.5, **p<0.01, ***p<0.001.

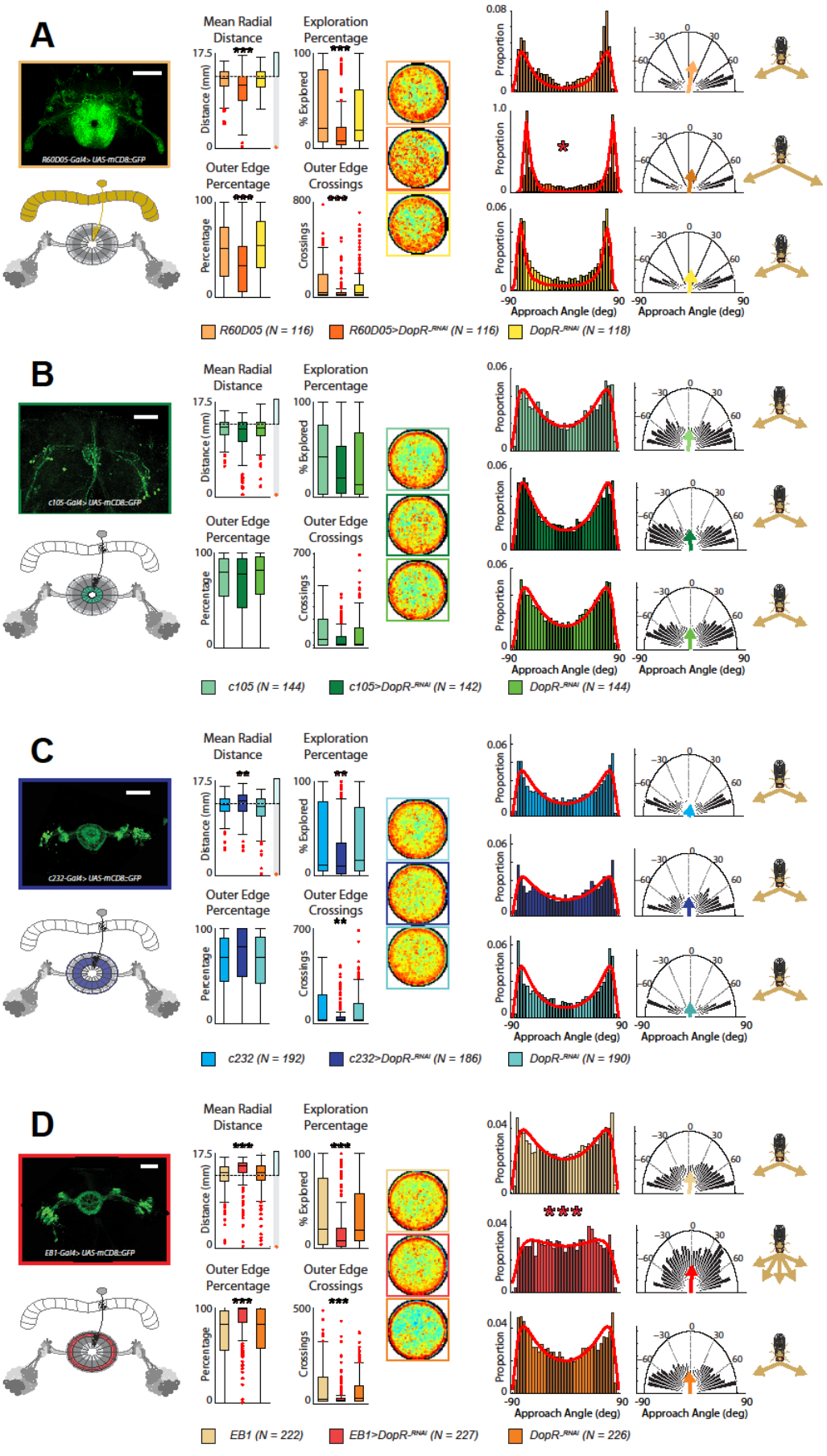
A
R60D05-Gal4> UAS-mCD8::GFP
Mean Radial Distance
Exploration Percentage
Outer Edge Percentage
Outer Edge Crossings
Distance (mm)
% Explored
Percentage
Crossings
Proportion
Approach Angle (deg)
R60D05 (N = 116)
R60D05>DopR-RNAi (N = 116)
DopR-RNAi (N = 118)
B
c105-Gal4> UAS-mCD8::GFP
c105 (N = 144)
c105>DopR-RNAi (N = 142)
DopR-RNAi (N = 144)
C
c232-Gal4> UAS-mCD8::GFP
c232 (N = 192)
c232>DopR-RNAi (N = 186)
DopR-RNAi (N = 190)
D
EB1-Gal4> UAS-mCD8::GFP
EB1 (N = 222)
EB1>DopR-RNAi (N = 227)
DopR-RNAi (N = 226)

Figure S3. *Dop1R1-*^{RNAi} expression affects open field exploration and turning behaviour in an ellipsoid body circuit-specific manner. Relates to Figure 3. (**A**) *R60D05-Gal4>Dop1R1-* ^{RNAi} place preference metrics and heatmap on the left; right turning behaviour for *R60D05-Gal4* control *R60D05-Gal4>Dop1R1-* ^{RNAi} and *Dop1R1-* ^{RNAi} control (**B**) *c105-Gal4>Dop1R1-* ^{RNAi} place preference metrics and heatmap on the left; right turning behaviour for *c105-Gal4* control, *c105-Gal4>Dop1R1-* ^{RNAi} and *Dop1R-* ^{RNAi} control. (**C**) *c232-Gal4>Dop1R1-* ^{RNAi} place preference metrics and heatmap on the left; right turning behaviour for *c232-Gal4* control, *c232-Gal4>Dop1R1-* ^{RNAi} and *Dop1R1-* ^{RNAi} control. (**D**) *EB1-Gal4>Dop1R1-* ^{RNAi} place preference metrics and heatmap on the left; right turning behaviour for *EB1-Gal4* control, *EB1-Gal4>Dop1R1-* ^{RNAi} and *Dop1R1-* ^{RNAi} control. All data are mean +/-SEM; *p<0.5, **p<0.01, ***p<0.001. Scale bar 50μm.

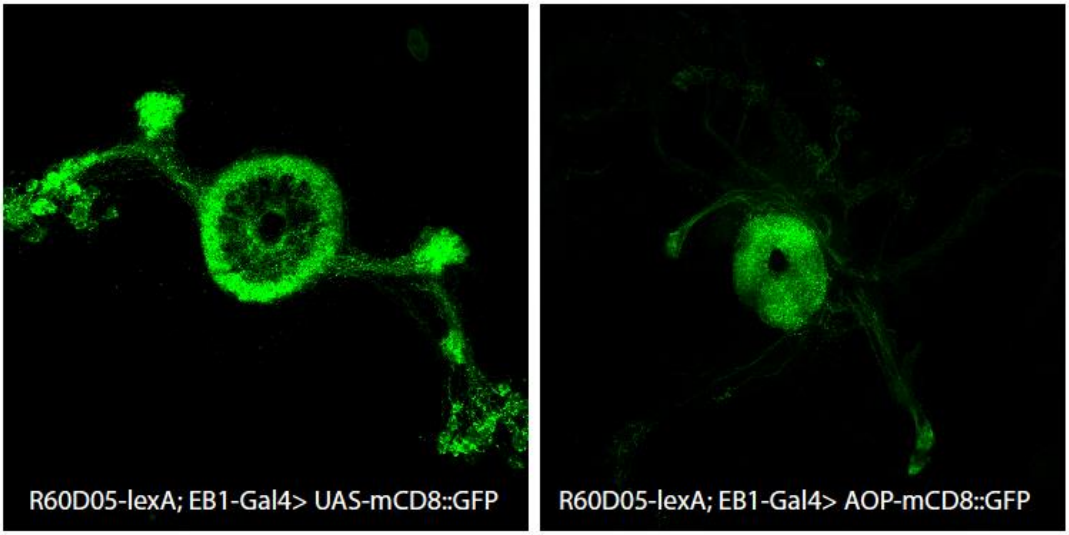

Figure S4. Brain-specific expression pattern of founder lines used for synaptobrevin-tagged Green fluorescent protein *reconstitution across* columnar wedge and tangential ring neurons. Relates to Figure 4. (Left) *R60D05-lexA; EB1-Gal4>UAS-mCD8::GFP* expression pattern highlight the ring neurons R2/R4m. (Right) *R60D05-lexA; EB1-Gal4>AOP-mCD8::GFP* highlight the columnar-wedge neurons innervating the ellipsoid body**.**

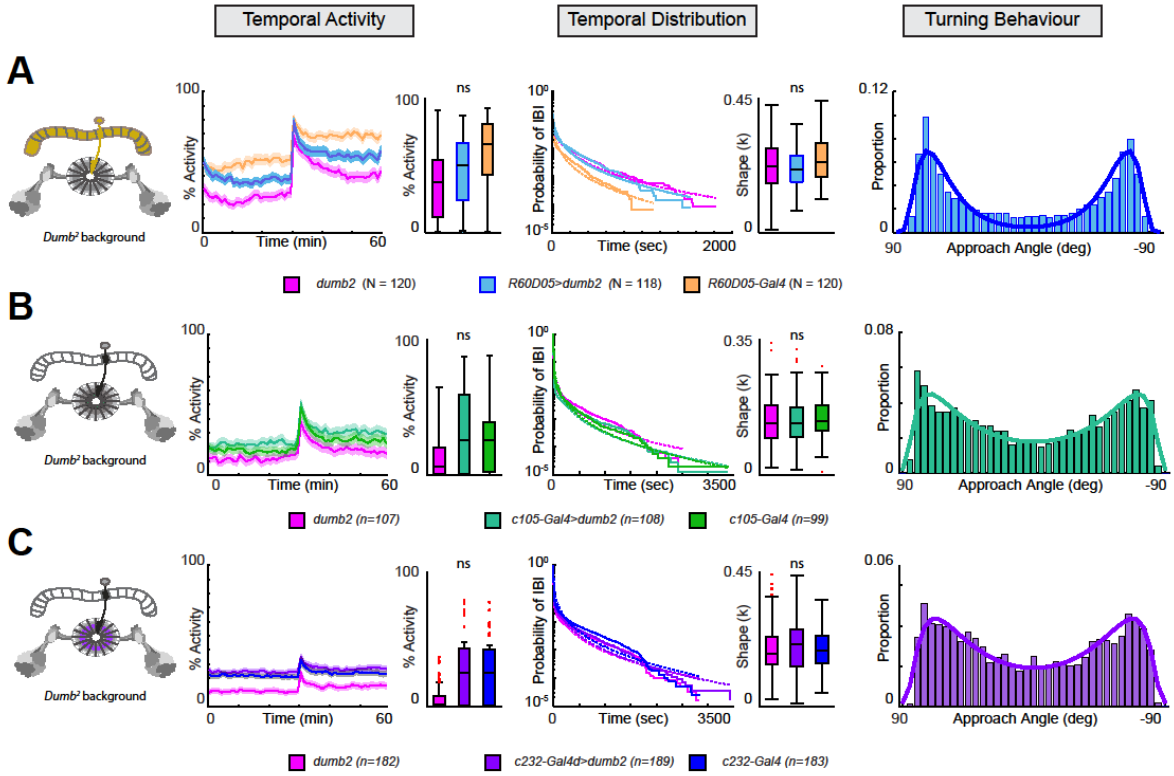

Figure S5. DopR1 receptor mutant Dumb2 affects activity levels but not temporal distribution of activity bouts or turning behaviour. Relates to Figure 5. Panels from left to right indicate DopR1 levels in entire brain and/or ring neuron subtype-specific ellipsoid body (EB) circuitry; temporal activity levels; mean activity; temporal distribution of inter-bout intervals (IBIs); shape factor κ of burstiness; distribution of approach angle for (**A**) *dumb*^{2} mutant compared to columnar-wedge specific driver *R60D05-Gal4* restoring Dop1R1 in *dumb*^{2} heterozygous background and *R60D05-Gal4* control flies (**B**) *Dumb*^{2} mutant compared to R1-specific *c105-Gal4* targeting Dop1R1 in *dumb*^{2} heterozygous background and *c105-Gal4* control flies; (**C**) *Dumb*^{2} mutant compared to R3/4d-specific *c232-Gal4* restoring Dop1R1 in *dumb*^{2} heterozygous background and *c232-Gal4* control flies. All data are mean +/-SEM; *p<0.5, **p<0.01, ***p<0.001.

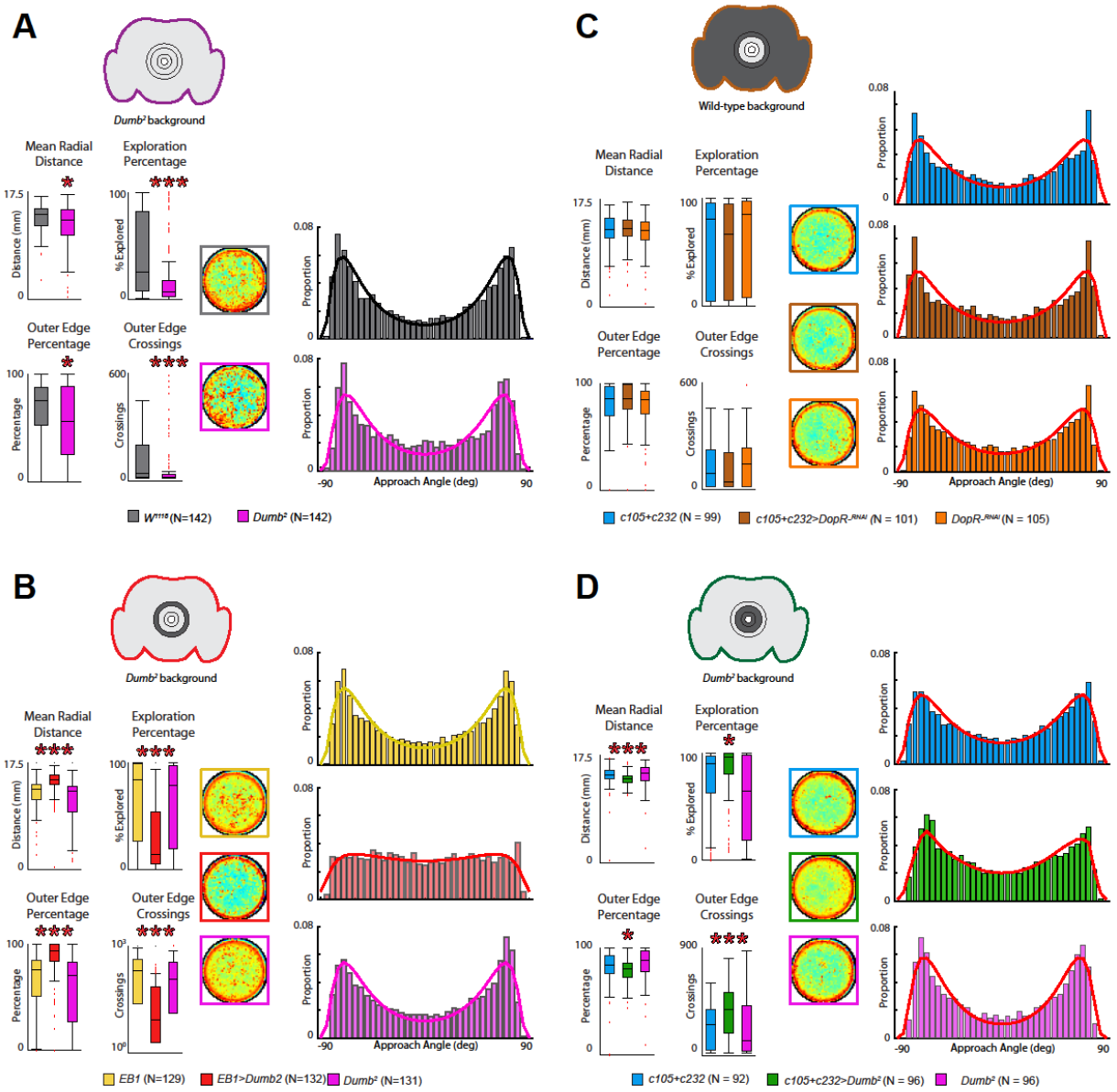

Figure S6. Place preference and exploration metrics for Dopaminergic manipulations. Relates to Figure 5. (A) *Dumb*^{2} place preference metrics and heatmap on the left shows less centrophobism; approach angle distributions between *w11118* and *dumb*^{2} on the right are not different. (**B**) R2/R4m specific *EB1-Gal4* restoring Dop1R1 in *dumb*^{2} heterozygous background show less centrophobism, less exploration and less transition from outer to inner edge region; right, altered turning behaviour for *EB1-Gal4> dumb*^{2}. (**C**) left, place preference metrics and heatmap for *c105-Gal4-c232-Gal4> Dop1R1-* ^{RNAi} and turning behaviour on the right. (**D**) left, place preference metrics and heatmap for *c105-Gal4-c232-Gal4> dumb*^{2} show a statistically significant decrease in centrophobism whereas turning behaviour, on the right, is not affected. All data are mean +/-SEM; *p<0.5, **p<0.01, ***p<0.001. Grey background represents low level of Dop1R1, whereas a darker background shows normal level of expression.